

Received November 30, 2018, accepted December 21, 2018, date of publication January 1, 2019, date of current version January 23, 2019.

Digital Object Identifier 10.1109/ACCESS.2018.2890335

Removal of Movement Artefact for Mobile EEG Analysis in Sports Exercises

EGLĖ BUTKEVI IŪTĖ¹, LIEPA BIKUL IENĖ¹, TATJANA SIDEKERSKIENĖ¹, TOMAS BLA AUSKAS², RYTIS MASKELIŪNAS², ROBERTAS DAMA EVI IUS^{1b2}, AND WEI WEI³, (Senior Member, IEEE)

¹Faculty of Mathematics and Natural Sciences, Kaunas University of Technology, 51368 Kaunas, Lithuania

²Faculty of Informatics, Kaunas University of Technology, 51368 Kaunas, Lithuania

³School of Computer Science and Engineering, Xi'an University of Technology, Xi'an 710048, China

Corresponding author: Tomas Blažauskas (tomas.blazauskas@ktu.lt)

This work was supported in part by the National Key Research and Development Program of China under Grant 2018YFB0203900, in part by the Key Research and Development Program of Shaanxi Province under Grant 2018ZDXM-GY-036, and in part by the National Natural Science Foundation of China under Grant 61572393, Grant 61877049, and Grant 11671317.

ABSTRACT We present a method for the removal of movement artifacts from the recordings of electroencephalography (EEG) signals in the context of sports health. We use a smart wearable Internet of Things-based signal recording system to record physiological human signals [EEG, electrocardiography (ECG)] in real time. Then, the movement artifacts are removed using ECG as a reference signal and the baseline estimation and denoising with sparsity (BEADS) filter algorithm for trend removal. The parameters (cut-off frequency) of the BEADS filter are optimized with respect to the number of QRS complexes detected in the reference ECG signal. Next, surrogate movement signals are generated using a linear combination of intrinsic mode functions derived from the sample movement signals by the application of empirical mode decomposition. Surrogate signals are used to test the efficiency of the BEADS method for filtering the movement-contaminated EEG signals. We provide an analysis of the efficiency of the method, extracted movement artifacts and detrended EEG signals.

INDEX TERMS Mobile EEG, movement artifact removal, sports e-health, digital signal processing.

I. INTRODUCTION

Service Oriented Architecture (SOA) systems for health monitoring are popular in health centers, clinics and smart home environments. These systems are used by elderly people, patients, sportsmen, etc. The electronic remote health monitoring systems sometimes can replace the conventional health care methods. However, the integration of the Internet of Things (IoT) into these systems can further increase interoperability, intelligence, and scalability [1]. A device which utilizes the IoT is uniquely addressed and can be identified anywhere and anytime through the Internet. The IoT based devices in smart health monitoring systems can connect and share the information with each other through the Internet automatically.

With the arrival of low-cost consumer-grade electroencephalogram (EEG) and electrocardiographic (ECG) devices, a large amount of data can be collected through IoT, smart wearables and Body Area Networks (BAN) and used for numerous e-health and well-being applications such as for workplace ergonomics [2], fatigue detection [3], epileptic seizure detection [4], tele-monitoring of chronic diseases [5],

activity recognition [6], depression monitoring [7], gaming [8], etc.

The collected data can be very useful for assessing human condition, but still requires effective computational intelligence algorithms to derive useful information in near real time. While ultimately only professional experts after lengthy inspection can conclude a medical diagnosis based on the available data, the average consumer requires instant feedback on his state and trends of well-being. Therefore, the development of automated expert systems to assist both professional experts and average users while analyzing large amounts of physiological data is very demanding for real-word e-health applications.

Analysis of human EEG during various motoric and imagery tasks is known to be useful for evaluating the links between neural system functions and behavior, and provides a straightforward measure of neural activity in real-time. EEG is captured using wired sensors attached to specific locations across the head. Recording brain surface activity during physical activities such as walking can provide useful knowledge to advance both neuroscience as well as sports health.

Moreover, capturing information about neural processes in real-time during daily activities could be used to improve Brain Computer Interface (BCI) systems. Having capability to record and analyze brain signal characteristics during real-world sports training rather than during artificially-setup laboratory tasks (as many other researchers do) are likely to lead to significant breakthrough in understanding how human body functions.

Currently, the users of BCI applications can make use of domestic-grade wearable headsets such as Emotiv (Hong Kong, ROC) and Neurosky (San Jose, CA, USA). These devices however are of limited use due to high noisiness of the recorded signals [9]. For psychophysiological monitoring and neurofeedback, smaller devices with a small number of electrodes such as B-Alert X series (Advanced Brain Monitoring, Carlsbad, CA, USA) and Neurobit Systems (Gdynia, Poland) exist. These gadgets were originally designed for personal use such as health monitoring and gaming instead of use in serious research.

With the increase of healthcare services in non-clinical environments the processing and analysis of wearable sensors are growing significantly [10]. The integration of smart multimodal interfaces, modeling and data mining techniques should guarantee that the developed system is comfortable and effective. Also, the dynamics and individual daily-life activities are important to human health. Electrocardiogram (ECG) analysis is commonly used and is known to be useful tool for screening a variety of heart diseases due to its simple application [11]. However, it has a high cost and long waiting time to meet a specialist for screening [12].

The EEG signals can be captured during sports activities when sportsmen are involved in regular sporting such as playing golf or riding a bicycle [13]. While there are obvious limitations for several kinds of sporting activities such as water-related (e.g. swimming) or high-impact sports such as rugby, there are no technical difficulties to record and monitor the EEG signals without any discomfort to a sporting person. For example, EEG was recorded outdoors while walking and fairly reliable single-trial P300 effects were observed by employing an auditory oddball task [14]. Wireless Emotiv headset with dry electrode sensors fitted into an elastic cap with an amplifier was successfully used while subjects walked freely outdoors [15].

However, the measurement and comprehension of brain surface signals during the execution of sports movement is plagued by noise and different artifacts due to the physical movement itself [16], [17]. According to [18], interpreting physiological data that includes semi-periodic or aperiodic movement artifacts such as originating from walking may be problematic. The recorded EEG signals, firstly, are contaminated by muscular activity artifacts, that are activated during motion tasks [19], [20]. The electromyography (EMG) artifacts are the most problematic to isolate from as their spectrum overlaps with EEG signal frequencies, mainly with beta and gamma waves [21]. Artifacts of other types such as occurring from sweat bridges, movements of cables and

electrodes, ballistocardiographic (BCG) artifacts, eye movements and blink artifacts also contribute significantly towards noisiness of the EEG signals. Electrode movement artifacts can be characterized by rapid change of impedance. BCG artifacts occur when the blood in veins induce a mechanical movement of the electrode placed directly on top of a blood vessel. Therefore, the main obstacle for a direct application of EEG recording and analysis during all the movement phases in sport still remain the movement artifacts [22].

Reliable capture of neural signals in active sporting environment can be tackled by the application of mathematical and signal processing methods (for a discussion, see [16]). For example, Independent Components Analysis (ICA) can segregate brain activity from movement artifacts. ICA uses the correlational manifold of signals to decompose brain signals into a set of statistically not-related components, which can be interpreted either as a physiologically meaningful signal or as a noise (see [23]). Using the ICA method, Gramann *et al.* [24] analyzed the event-related potentials (ERPs) captured on a treadmill, while standing, slow or fast walking, and running. The ocular and muscular artifacts have been separated from the EEG signals using blind source separation (BSS) techniques [25], such as canonical correlation analysis (CCA) [26], but they have not been efficient with movement artifacts present due to the correlation between noise signals. Moreover, artifact subspace reconstruction (ASR) [27] has also been applied to filter out artifacts from the EEG signals.

In this context, the development of methods and systems that can extract the actual movement artifacts and reject (subtract) them from the original EEG signals is highly relevant for sports medicine and e-health applications. We present a method for the removal of movement artifacts from the recorded electroencephalography (EEG) signals in sports health. We use a smart wearable signal recording system to record the physiological human signals (EEG, electrocardiography (ECG)) in real-time. Then the movement artifacts are removed using ECG as a reference signal and Baseline Estimation and Denoising with Sparsity (BEADS) filter algorithm [28] for trend removal. Next, surrogate movement signals, are generated using a linear combination of Intrinsic Mode Functions (IMF) derived from the sample movement signals using Empirical Mode Decomposition (EMD), are used to test the efficiency of the BEADS method for filtering movement-contaminated EEG signals. We provide an analysis and comparison of the extracted movement artifacts and detrended EEG signals.

The organization of other parts of the paper is as follows. Section II describes the monitoring architecture, methods and materials used, including BEADS and surrogate generation method. Section III provides the results of experiments. Section IV formulates the conclusions.

II. METHODS AND MATERIALS

A. OVERVIEW OF METHODOLOGY

We assume that the ECG and EEG signals registered during the physical movement of a human are contaminated with

both high and low frequency noise and artifacts. Before baseline detection and its elimination, the noise suppression should be done. Almost all high pass filtering methods have sharp cut-off frequencies, which in many cases distort the raw signal [29]. Using wavelet based techniques for high-frequency noise removal from the physiological signals requires numerous experiments for finding different parameters and thresholds [30]. Other most common methods like Fast Fourier Transform (FFT) [31] or Finite Impulse Response (FIR) filter [32] techniques are limited. They fail to discover the exact location of frequency components in time. For the real time calculations, it is important that all methods would be as low time consuming as possible. However, high-pass filtering should not damage the original signal and ensure that main signal characteristics remain the same. The problem with the EEG signals is that their waveforms do not have a characteristic and easily recognizable shape form (i.e., QRS complex) like the ECG signals have. Therefore, it is difficult to evaluate the efficiency of filtering of the EEG signals compared to the ECG signals. Therefore, we use the ECG signals derived during physical motion as reference signals for constructing an optimal filter for movement artifact removal. Then the optimized is applied onto the EEG signals.

The outline of our methodology is presented in Figure 1 and is detailed below.

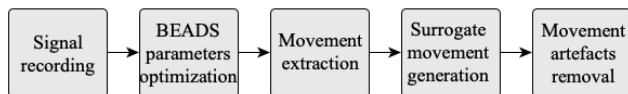


FIGURE 1. Service Oriented Architecture of the system components.

(1) Recording of signals: ECG and EEG signals during a series of physical exercises are recorded using Service-Oriented Architecture (SOA) for monitoring of human physiological signals (originally described in [33]).

(2) Optimization of the BEADS filter parameters (cut-off frequency) using the artifact-contaminated ECG signal as a reference and the number of detected QRS complexes as a fitness function.

(3) Extraction of the movement signals using an optimized BEADS filter.

(4) Generation of the surrogate movement signals using Intrinsic Mode Functions (IMFs) derived by Empirical Mode Decomposition (EMD) [34].

(5) Removal of the movement artifacts from the movement-contaminated EEG signals.

The flow chart of the proposed method is shown in Figure 2 as follows: 1) ECG high-frequency noise reduction, 2) Trend extraction from electrocardiogram, 3) Baseline appliance on EEG signal, 4) EEG signal low-band filtering and 5) result comparison.

Before baseline detection and its extraction, additional normalized cut-off frequency analysis was made. For the estimation of best filter parameter the QRS complex searching algorithm was implemented, and the number of QRS complex

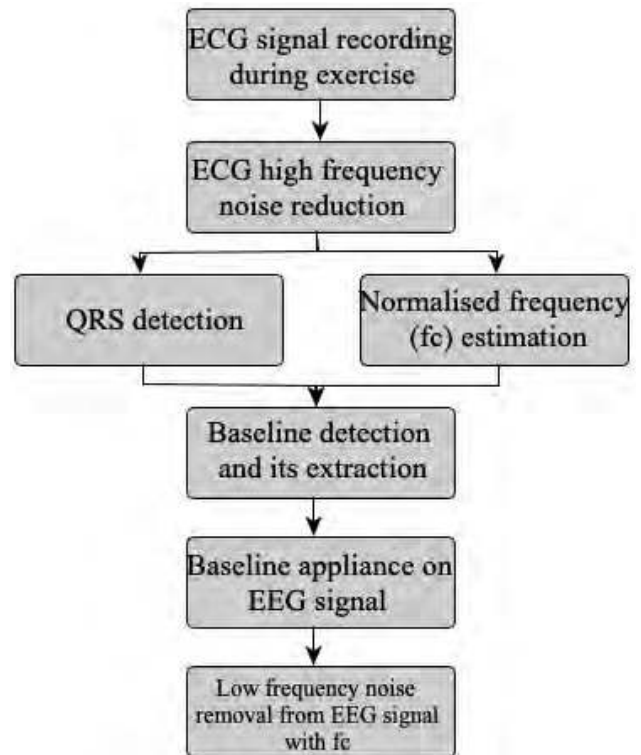


FIGURE 2. Schematical diagram of applied methods.

detected used as a fitness function for optimization. The ECG high-frequency noise is removed using the median filter, while for the baseline detection, the BEADS algorithm was applied.

B. SERVICE ORIENTED ARCHITECTURE FOR HUMAN PHYSIOLOGICAL SIGNAL MONITORING

The IoT-based implementation of the ECG monitoring system which includes cloud based signal processing was adopted (see Figure 3). It consists of the following functional units:

(1) Electrocardiography device (Cardiograph) with its sensors enabled to capture the ECG signal and provide information to a logging device located nearby using the Bluetooth wireless connection;

(2) The logging device (smartphone), which collects information from ECG and other sensors and transmits it to a remote computer (cloud server);

(3) The remote computer, which receives, stores, analyses the data and provides feedback as a cloud service.

C. BASELINE ESTIMATION AND DENOISING WITH SPARSITY (BEADS) ALGORITHM

1) BEADS ALGORITHM

The linear filters with fixed cut-off frequencies often cannot identify useful information from the ECG waveform and baseline wander components become hard to remove completely [35]. The trend in the ECG signal is interpreted as a

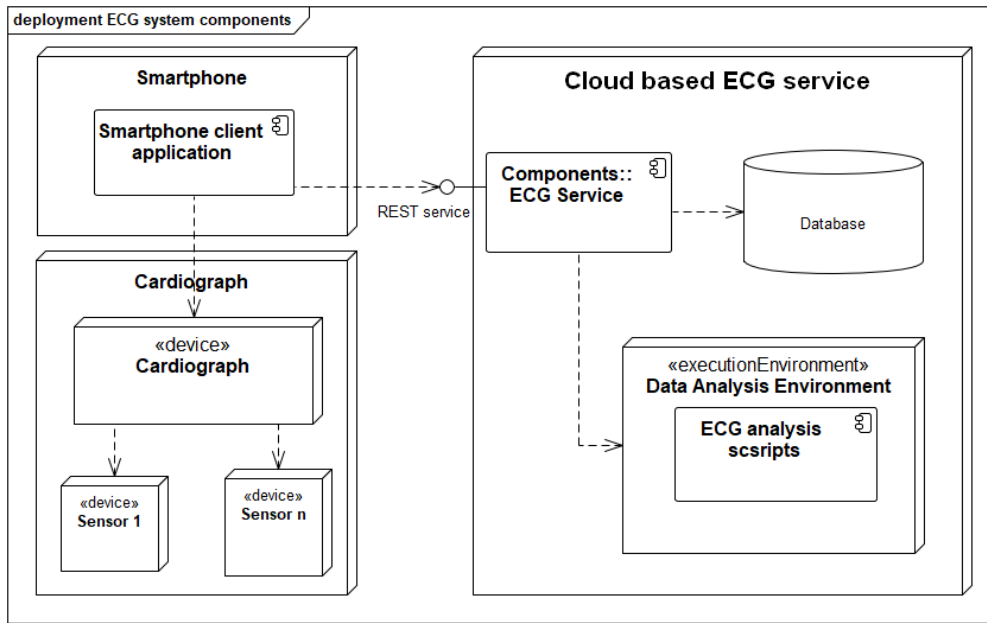


FIGURE 3. Service Oriented Architecture of the Human Physiological Signal Monitoring system components.

low frequency noise. If a person is in stationary condition, the trend of the ECG signal is low, and it could be removed using low-order polynomial methods. In some cases, the data could be subtracted from each time-series signal objects. However, in the context of active sports training exercises, the trend is not stationary or linear and can be considered as a low-frequency noise.

The noisy ECG data can be modeled as:

$$y(n) = f(x) + v(x) + w(x), \quad x = 0, \dots, N - 1 \quad (1)$$

where f is a low-pass signal, w is a stationary white Gaussian noise and v is a sparse-derivative signal [36]. For the data described in (1) it is not suitable to use neither sparsity-based de-noising methods, nor low-pass filtering. However, a combination of these two methods is suitable. The N point signal can be defined as:

$$x = [x_0, x_1, \dots, x_{N-1}]^T. \quad (2)$$

The high-pass filter H passes signals with a frequency higher than a cut-off frequency and attenuates signals with frequencies lower than the cut-off frequency. It can be characterized by its transfer function as shown below:

$$H(x) = \frac{B(x)}{A(x)} = \frac{b_0 + b_1x^{-1} + b_2x^{-2} + \dots + b_Nx^{-N}}{1 + a_1x^{-1} + a_2x^{-2} + \dots + a_Nx^{-N}} \quad (3)$$

where order of the filters is the greater than N [37].

The low pass filter L can be defined as (4), where I is a diagonal matrix with ones on the main diagonal and zeros elsewhere:

$$L = I - H \quad (4)$$

The combination of the conventional low-pass filtering and sparsity-based de-noising usually requires time consuming calculations due to its complexity [38]. The baseline estimation and de-noising with sparsity algorithm (BEADS) [28] removes the trend from the data using baseline (or low-frequency noise wave) detection and removal. The filters (as defined in (3) and (4)) L and H are taken with zero-phase, recursive and non-causal. The filter parameters are its order and its cut-off frequency. Design of the filter requires the definition of first and second order difference matrixes.

The first-order difference matrix $(N - 1) \times N$ is defined as:

$$A = \begin{bmatrix} a_0 & a_1 & & & & \\ a_1 & a_0 & a_1 & & & \\ & a_1 & a_0 & a_1 & & \\ & & a_1 & a_0 & a_1 & \\ & & & a_1 & a_0 & a_1 \\ & & & & a_1 & a_0 \end{bmatrix}; \quad (5)$$

where a_0 and a_1 are filtering coefficients.

The second-order difference matrix $(N - 2) \times N$ is:

$$B = \begin{bmatrix} -1 & 2 & -1 & & & \\ & -1 & 2 & -1 & & \\ & & -1 & 2 & -1 & \\ & & & -1 & 2 & -1 \\ & & & & -1 & 2 & -1 \end{bmatrix}. \quad (6)$$

If $D_0 = I$, where I is the identity matrix and $D_1 = A$, $D_2 = B$, then the difference operator of order k (of size $(N - k) \times N$) can be denoted as D_k .

To evaluate positive and negative ECG peaks, the asymmetric penalty function $\theta(x_n; r)$ is constructed, here r is an asymmetric parameter.

The algorithm solves the problem written below:

$$\hat{x} = \arg \min_x \left\{ \frac{1}{2} \|H(y - x)\|_2^2 + \lambda_0 \sum_{n=0}^{N-1} \theta(x_n; r) + \sum_{i=1}^M \lambda_i \sum_{n=0}^{N_i-1} \varphi([D_i x]_n) \right\}, \quad (7)$$

where φ is a differentiable symmetric penalty functions, λ_i are regularization parameters, and the norm is defined as:

$$\|x\|_2^2 = \sum_n |x_n|^2. \quad (8)$$

If the function $g(x, v)$ is taken of the form

$$g(x, v) = ax^2 + bx + c \quad (9)$$

which is an upper bound of function θ and $x = v$, $x = s$, are values close to zero from both sides then solving differentiation equations with respect to the first argument gives the result:

$$a = \frac{1+r}{4|v|}, \quad b = \frac{1-r}{2}, \quad c = \frac{(1+r)|v|}{4}, \quad s = -v. \quad (10)$$

These values are put into the equation (3) and the $g(x, v)$ function gains the form:

$$g(x, v) = \frac{1+r}{4|v|}x^2 + \frac{1-r}{2}x + \frac{(1+r)|v|}{4} \quad (11)$$

With the same parameter the $\Gamma(v)$ function can be defined as:

$$\Gamma(v) = \begin{cases} \frac{1+r}{4|v|}, & |v| \geq \varepsilon; \\ \frac{(1+r)}{4}, & |v| < \varepsilon. \end{cases} \quad (12)$$

The cost function $G(x, v)$ is defined as:

$$G(x, v) = \frac{1}{2} \|H(y - x)\|_2^2 + \lambda_0 x^T [\Gamma(v)]x + \sum_{i=0}^M \left[\frac{\lambda_i}{2} (D_i x)^T [\Lambda(D_i v)] (D_i x) \right] + c(v), \quad (13)$$

where $\lambda_i \geq 0$ are regulation parameters, $c_i(v)$ are scalars, D_i is the order - i difference operator.

$$[\Lambda(D_i v)]_{n,n} = \frac{\varphi'(v_n)}{v_n}. \quad (14)$$

Moreover, using the commutative property of linear, time-invariant systems, a high pass filter H is defined as

$$H = BA^{-1}, \quad (15)$$

where A and B represent linear, time-invariant (LTI) systems, and H is a cascade of LTI.

Minimizing the cost function $G(x, v)$ with respect to x leads to (16) solution. The parameters are recalculated until the best (with the lowest residuals) baseline is found [39].

$$x = \left(H^T H + 2\lambda_0 \Gamma(v) + \sum_{i=0}^M \lambda_i D_i^T [\Lambda(D_i v)] D_i \right)^{-1} H^T H y = A Q^{-1} B^T B A^{-1} y, \quad (16)$$

where $Q = B^T B + A^T \left(\sum_{i=0}^M \lambda_i D_i^T [\Lambda(D_i v)] D_i \right) A$.

Note that in some cases, the BEADS algorithm has long lasting calculation time, because it contains the inverse matrix estimation and matrixes with values close to zero requires more time. However, this method has linear complexity which, in total, leads to a good computational result.

2) QRS COMPLEX DETECTION

As it was mentioned in the previous paragraphs, the ECG signal is used to measure the heart rate, respiration and regularity of heartbeats. It shows the size, activity and position of heart chambers. The ECG signal has a distinct and characteristic shape contained with different waves, which is shown in Figure 4. The QRS complex is made by contraction of the left and right ventricles. It contains the Q, R and S waves, which involves more muscle mass and are stronger than P or T waves. That is why it has larger fluctuation in the graph [40].

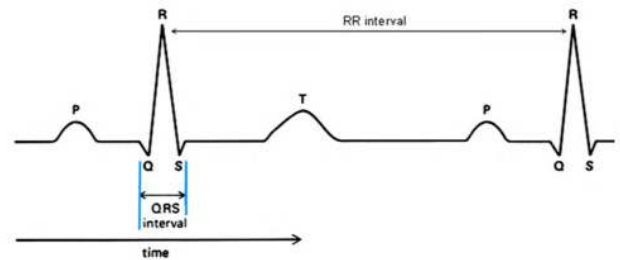


FIGURE 4. Typical shape of QRS complex.

To estimate the filtering parameters, it is important to have certain criterions that would allow to identify if an algorithm works properly and with acceptable errors. One of these criterions could be the root mean square error (RMSE) or any other error measure. However, it could lead to the elimination all or a part of signal parameters. To avoid information losses during filtering, we have selected the QRS complex detection [40] as a fitness function. The method is based on the detection Q, R and S waves in ECG signal and calculation of the number of QRS complexes. We assume that the more QRS complexes are found in the analysed ECG signal the better is the filtering algorithm. It is not hard to notice that if at least one wave (Q, R or S) is not identified, the QRS complex also cannot be found.

The QRS complex detection method is based on the motor unit action potentials (MUAPs) analysis [41]. The first step of this algorithm is to detect the initial set of MUAPs in

the noisy ECG recording. To make sure that there is no noise of power-line interfaces the narrow-band notch filter is applied by removing the 50 Hz frequency [41]. After signal processing, the peak detection is applied. The most visible wave in the ECG signal is the R-wave. That is why the first ECG signal processing task is the recognition of the R-wave. Then the QRS complex and other ECG parameters can be found. The recognition of the QRS complexes (Figure 4) includes finding their position in time and the time interval between them [42].

There are many methods, which can be used for the QRS complex detection like neural networks [43], wavelet transform [44], filter banks [45], adaptive filters, genetic algorithms, Hidden Markov Models (HMM), mathematical morphology operators, Hilbert, length and energy transformations, and syntactic methods. Most of these methods require large computing resources, or have a big delay, or are sensitive to noise and sudden signal change. To avoid these disadvantages, we used the QRS detection method based on the Pan-Tomkins algorithm [37], which uses the calculation of the signal derivatives.

For optimization of the BEADS filter parameters we use Algorithm 1:

Algorithm 1

Inputs: Movement-contaminated ECG signal

Output: Parameters of BEADS filter

BEGIN

for each BEADS parameter do

$best_value = 0;$

$maxQRS = 0;$

 for each $parameter_value$ do

 detrrend ECG signal using BEADS algorithm;

 find R , Q and S peaks;

$j = 1;$

 for i from 1 to $\max(\text{length}(R), \text{length}(Q),$

$\text{length}(S))$ do

 if $Q(i)$ or $R(i)$ or $S(i)$ is empty

$i = i + 1;$

 else

$QRS(j) = \text{estimate QRS complex};$

$j = j + 1;$

 if $maxQRS < \text{length}(QRS)$

$maxQRS = \text{length}(QRS);$

$best_value = parameter_value;$

 END

3) EXTRACTION OF MOVEMENT SIGNALS AND REMOVAL OF MOVEMENT ARTIFACTS

After the BEADS algorithm is applied, low frequency noise (baseline) is estimated and subtracted from the ECG signal. This baseline can be interpreted as movement artifact. However, it can still correlate with the ECG signal. That is why additional decorrelation is applied to reduce

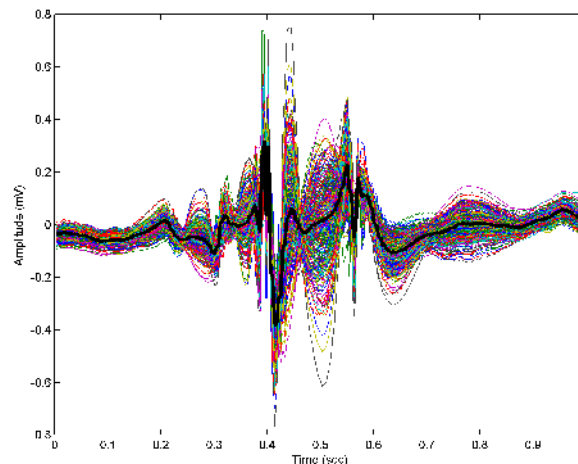


FIGURE 5. Sample movement signal (bold black) and its surrogates.

correlation within an ECG signal, while preserving the baseline.

4) GENERATION OF SURROGATE MOVEMENT SIGNALS

Surrogate data refers to time series data that is produced using well-defined models that reproduce signal spectrum [46] or various statistical properties of an original data [47]. Surrogate data may be used to supplement available data and used for recognizing patterns not seen in original data, developing and analyzing data models [48] or improving data classification of forecasting. Surrogate data can be produced in many ways, e.g., through statistical processes [47], which may involve random data generation using constraints of the model or system [48] or by assuming random phases and taking the inverse FFT of the given periodogram. Here for surrogate movement signal generation we propose using Intrinsic Mode Functions (IMF) derived by Empirical Mode Decomposition (EMD), an empirical data-driven technique for signal decomposition [34]. The IMFs represent a set of almost orthogonal functions with varying amplitude and frequency, which could be assigned a physical meaning. Many variants and extensions of EMD exist such as weighted sliding EMD, Ensemble EMD (EEMD), Complete Ensemble EMD with Adaptive Noise (CEEMDAN), which were proposed to address the main issues of EMD such as mode mixing and the boundary problem. The computational complexity of these improved methods is, however, higher and mode mixing is not important for us, since we sum mixed IMFs, if any, back to obtain surrogate signals, while the boundary problem can be solved by truncating the surrogate signal. Therefore, we have selected the classical EMD method, which has a well researched behavior, for further use. As a result of the application of EMD, the orthogonal IMFs are obtained from which the original signal $x(t)$ may be reconstructed as follows:

$$x(t) = \sum_i IMF_i(t) + E(t). \quad (17)$$

here E is the residue error.

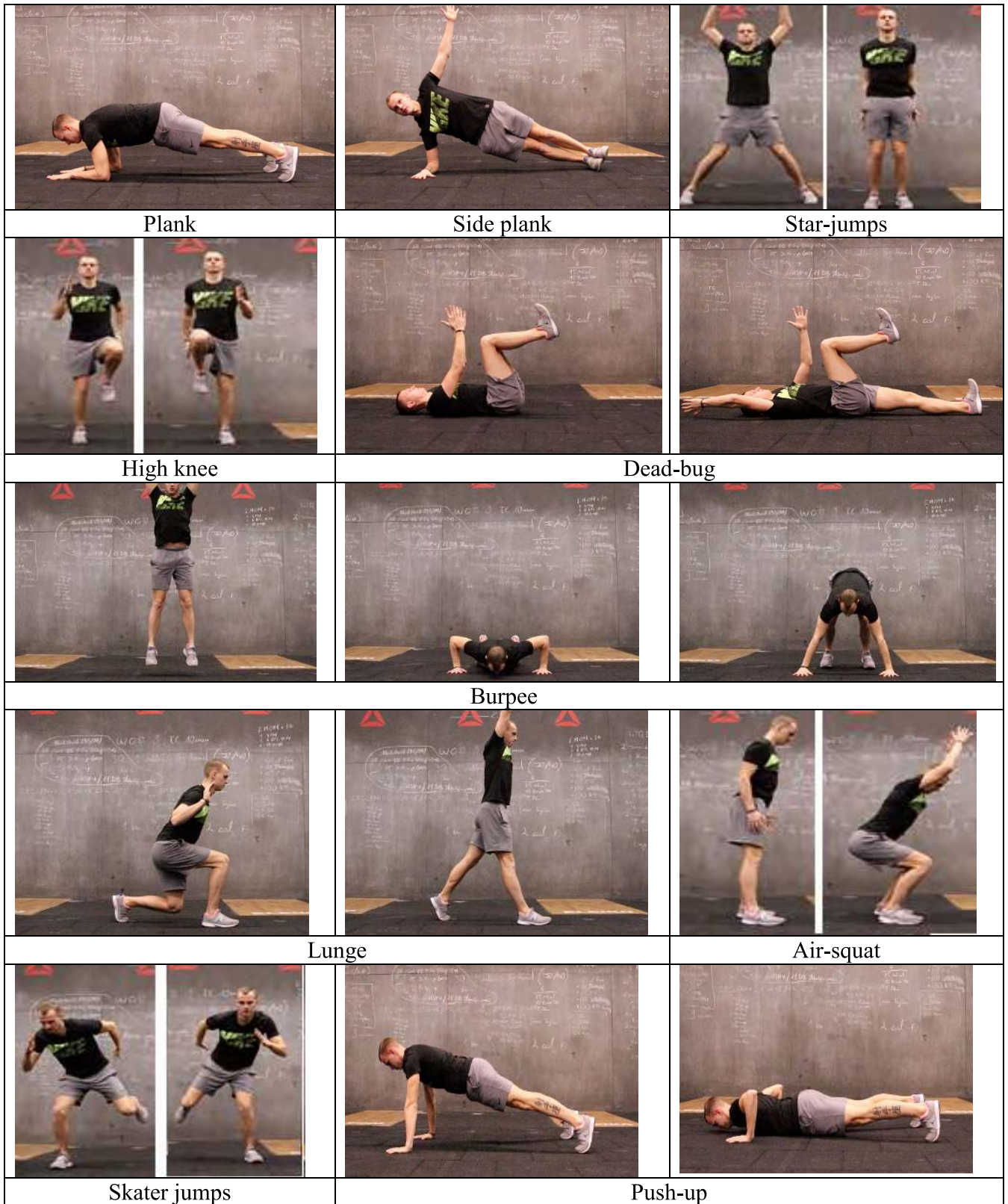


FIGURE 6. Physical exercises performed during our experiments.

In matrix form, the decomposition can be written as

$$X = I \cdot IMF \tag{18}$$

here I is the identity matrix.

The surrogate data series are generated as a randomly weighted sum of IMFs as follows:

$$\tilde{X} = n \frac{R}{\sum R} \cdot IMF \tag{19}$$

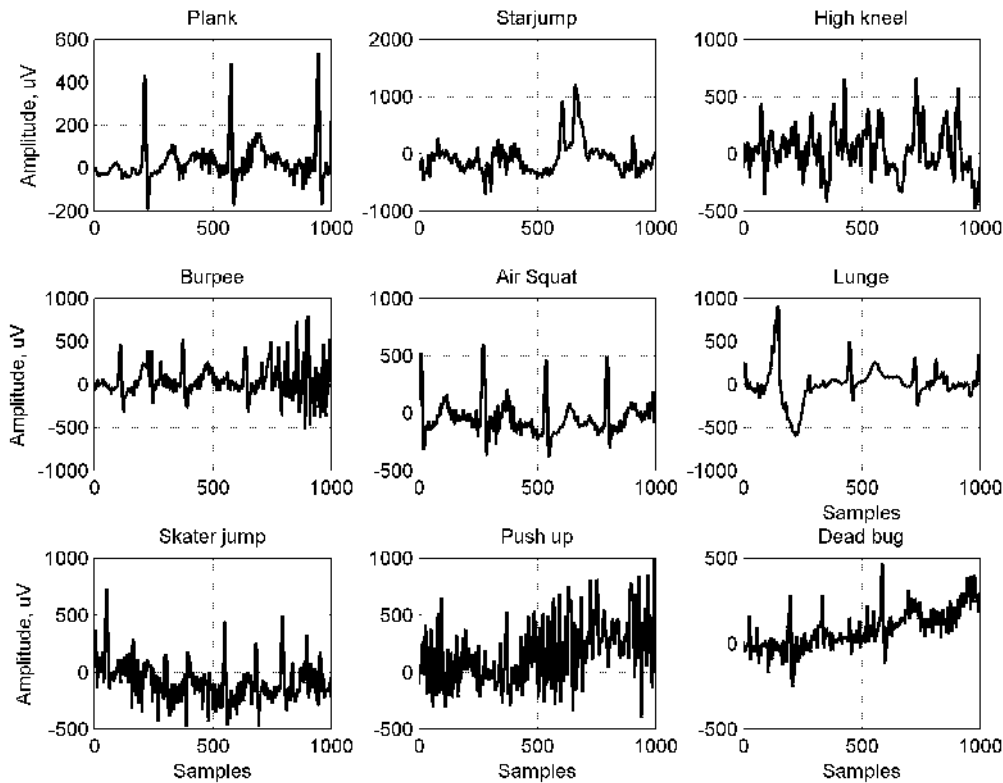


FIGURE 7. Samples of signals registered during the physical exercises.

here \tilde{X} is the surrogate signal, R is the uniformly distributed random vector, and n is the number of IMFs.

The result for a sample movement signal is illustrated in Figure 5, the surrogate signals are shown alongside the reference movement signal.

5) PERFORMANCE EVALUATION

The evaluation of the results is a crucial step to demonstrate the reliability and accuracy of the proposed method. In validation, the performance indices are computed between the reconstructed and known original values. We evaluate the accuracy of the results using *Pearson correlation coefficient*, which estimates the strength and direction of the linear relationship between two variables:

$$R^2 = \frac{\{\sum (x_i - \bar{x})(y_i - \bar{y})\}^2}{\sum (x_i - \bar{x})^2 \sum (y_i - \bar{y})^2}. \quad (20)$$

here x_i, y_i are the individual sample points with index i ; and \bar{x}, \bar{y} are the averaged values of the samples.

In our case, we use the spectral correlation of signals, which is calculated as follows:

$$R_{sp}^2 = \frac{\{\sum (S_f(x) - \bar{S}(x))(S_f(y) - \bar{S}(y))\}^2}{\sum (S_f(x) - \bar{S}(x))^2 \sum (S_f(y) - \bar{S}(y))^2}, \quad (21)$$

here $S_f(x), S_f(y)$ are the amplitude spectra values (in dB) of signals x, y at frequency f , respectively, and $\bar{S}(x), \bar{S}(y)$ are the averaged spectrum values of x and y .

III. DATA AND RESULTS

A. EXPERIMENTAL SETTING

We used CardioScout Multi-ECG device for recording of ECG signals (sampling frequency 500 s^{-1}). The ECG and EEG signals were taken when a person walked and performed a set of ten main functional training exercises [49]. This set consist of two static exercises: plank and side plank (working muscles: core, shoulder, back), two cardio exercises: star-jumps and high knee (working muscles: hands, legs), and six dynamical exercises: dead-bug (working muscles: core, shoulder mobility, hip flexors), burpee (multifunctional), lunge, air-squat and skater jumps (working muscles: legs, buttocks) and push-up (core, back, chest). Duration of each exercise performance was 1 min. Figure 6 demonstrates the exercises schematically. The samples of ECG signals registered during the physical exercises are shown in Figure 7. The recorded ECG signals have various amplitudes and wave forms, because they have been affected by different high and low frequency noise.

We have performed all computations and processing of signals using customized MATLAB scripts.

B. RESULTS OF BEADS OPTIMIZATION

The optimization of the BEADS filter parameters was applied following the procedure described in Section 2. An example of the process optimization with the parameter value of cut-off frequency f_c applied on the ECG signal during the different exercises will be shown further. Each exercise has its own baseline because different muscles are working. How-

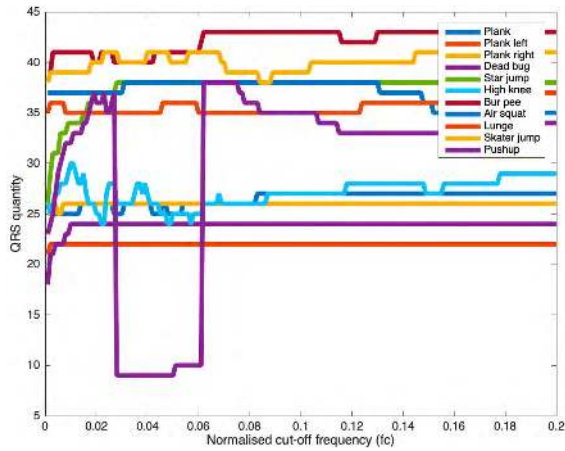


FIGURE 8. Normalized cut-off frequencies in different physical exercises for detection of QRS complexes in movement artifact contaminated ECG signals.

ever, the best results are reached with $f_c < 0.1$ (see Figure 8). Some exercises are almost stationary (plank, side plank) and their best normalized frequency is a small value ($f_c < 0.02$), because there is little trend to remove. Meanwhile, cardio exercises (like high knee or skater jump) have larger trend and are more affected with high-frequency noise. That is why the QRS detection becomes a complicated task and f_c values are fluctuating more.

During the ECG signal processing and its trend removal, the QRS detection process is initialized in each step. We assume that the more QRS complexes are found the better result is reached. By repeating this cycle, the best normalized cut-of frequency (f_c) of the BEADS filter is found. This parameter is important for the trend analysis and its removal. The example of the number of QRS complexes with respect to different normalized frequencies is shown in Figure 8.

For the ECG signal filtering, two methods were applied. The median filter was used to reduce high-frequency noise and the BEADS algorithm was used to remove a trend from the signal. We noticed that the “dead bug” exercise has a high trend, which fluctuates a lot. The example of this exercise is represented in Figure 9. After the ECG signal pre-processing is complete and all trends obtained, the next step is a baseline application on the EEG signal. Simulated EEG signals were modeled as a superposition of two components: the original EEG signals and the surrogate movement signals generated from the original movement signals that were extracted from the movement-contaminated ECG signals by the application of the BEADS algorithm. This allowed us to simulate removal of movement artifact from the EEG signal during physical exercises.

The spectral Pearson’s correlation (Eq. 21) was estimated using the spectra of the original and simulated EEG signal (after baseline removal) (see Table 1). For better comparison the alpha beta and gamma waves were separated, and their spectrum correlation was calculated. Here $spcorr_{sig}$ shows the spectrum correlation of the original and detrended EEG

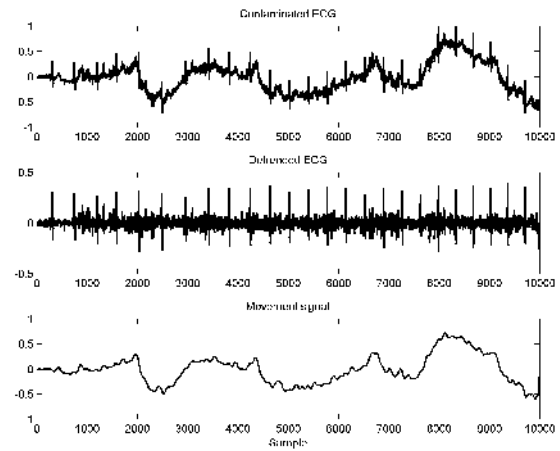


FIGURE 9. Example of the ECG signal contaminated with movement artifacts (top), detrended ECG signal (middle), and extracted movement signal (bottom).

TABLE 1. Correlation of original EEG signal and the movement-contaminated EEG signal after removal of movement artefacts.

Physical exercise	$spcorr_{sig}$	$spcorr_{alpha}$	$spcorr_{beta}$	$spcorr_{gamma}$	$best_{f_c}$
Plank	0.895	0.908	0.929	0.931	0.083
Plank left	0.900	0.948	0.958	0.962	0.002
Plank right	0.907	0.954	0.963	0.963	0.003
Dead bug	0.923	0.920	0.954	0.963	0.010
Star jump	0.930	0.962	0.974	0.964	0.028
High knee	0.914	0.930	0.969	0.966	0.010
Bur pee	0.902	0.924	0.957	0.950	0.062
Air squat	0.928	0.958	0.972	0.960	0.031
Lunge	0.836	0.849	0.871	0.869	0.167
Skater jump	0.920	0.867	0.942	0.949	0.023
Push up	0.923	0.916	0.960	0.963	0.062

signals, while $spcorr_{alpha}$, $spcorr_{beta}$, $spcorr_{gamma}$ represent the spectrum correlation between the alpha (8-15 Hz), beta (16-31 Hz), and gamma (≥ 32 Hz) waves of EEG, respectively, and $best_{f_c}$ corresponds to the best cut-off frequency that is used for the filtering of the EEG signal.

The spectral correlation coefficients presented in Table 1 indicate that the proposed method does not damage the spectral characteristics of the EEG signal thus the denoised signal resemble the original signals. Best correlation was achieved when the subjects performed Star jumps and Air squat exercises. The results were obtained using normalized frequencies of 0.010 and 0.031, respectively. Higher frequencies lead to lower Pearson correlation (see exercise “Lunge” in Table 1). This could have happened at the time of trend removal, because of the corruption of the signal. The higher the frequency is, the more corruption to the signal is done, because the EEG signal mainly has the higher frequency waves.

As a metric of efficiency of the movement artifact removal, we also use the Pearson correlation (Eq. 20) between the movement signal and the detrended EEG signal. The results for different types of physical exercises are shown in

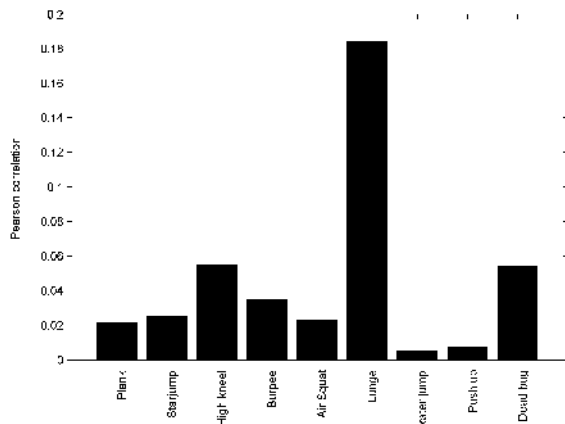


FIGURE 10. Pearson correlation between the movement signal and the detrended EEG signal.

Figure 10. The bar plot shows that there is low correlation between the movement signal and the detrended EEG signal, which means that the signal separation worked quite well.

IV. CONCLUSION

The removal of movement artifacts from the recordings of physiological signals during the dynamic activities of human behavior is important for analyzing and understanding the way a human body works. In this paper we have created a novel approach for removing the movement artifacts from the recordings of electroencephalography (EEG) signals.

We have applied the BEADS algorithm with adaptive parameters to identify and extract the movement-related signals using the recorded electrocardiography (ECG) signals as a reference. When applied to the movement-contaminated EEG signals we have managed to successfully reduce the movement-related artefacts. We have examined the efficiency of our approach on a variety of artificially generated surrogate movement signals obtained from the extracted movement signals by random mixing of independent signal modes (i.e., Intrinsic Mode Functions - IMF) derived by applying Empirical Mode Decomposition (EMD). The results were evaluated using Pearson correlation and spectral Pearson correlation.

The results of experiments performed with 11 types of physical exercises show that the proposed movement artifact removal method allowed to successfully remove movement artifacts while preserving the spectral characteristics of the EEG signal both in its entirety (spectral correlation: 0.836 – 0.930) as well as in different EEG signal bands (alpha: 0.849 – 0.962, beta: 0.871 – 0.974, gamma: 0.869 – 0.966).

In future work, we plan to extend our work to other types of human activities and recorded signals in the context of Assisted Living Environments.

REFERENCES

[1] A.-M. Rahmani et al., “Smart e-health gateway: Bringing intelligence to Internet-of-Things based ubiquitous healthcare systems,” in *Proc. 12th Annu. IEEE Consum. Commun. Netw. Conf. (CCNC)*, Jan. 2015, pp. 826–834, doi: [10.1109/ccnc.2015.7158084](https://doi.org/10.1109/ccnc.2015.7158084).

[2] V. Raudonis, R. Maskeliūnas, K. Stankevičius, and R. Damaševičius, “Gender, age, colour, position and stress: How they influence attention at workplace?” in *Computational Science and Its Applications—ICCSA*. Cham, Switzerland: Springer, 2017, pp. 248–264, doi: [10.1007/978-3-319-62404-4_19](https://doi.org/10.1007/978-3-319-62404-4_19).

[3] M. Ulinskas, M. Wo niak, and R. Damasevicius, “Analysis of keystroke dynamics for fatigue recognition,” in *Computational Science and Its Applications—ICCSA*. Cham, Switzerland: Springer, 2017, pp. 235–247, doi: [10.1007/978-3-319-62404-4_18](https://doi.org/10.1007/978-3-319-62404-4_18).

[4] K. Vandecasteele et al., “Automated epileptic seizure detection based on wearable ECG and PPG in a hospital environment,” *Sensors*, vol. 17, no. 10, p. 2338, 2017, doi: [10.3390/s17102338](https://doi.org/10.3390/s17102338).

[5] C. Wen, M.-F. Yeh, K.-C. Chang, and R.-G. Lee, “Real-time ECG telemonitoring system design with mobile phone platform,” *Measurement*, vol. 41, no. 4, pp. 463–470, 2008, doi: [10.1016/j.measurement.2006.12.006](https://doi.org/10.1016/j.measurement.2006.12.006).

[6] R. Damaševičius, M. Vasiljevas, J. Šalkevičius, and M. Wo niak, “Human activity recognition in AAL environments using random projections,” *Comput. Math. Methods Med.*, vol. 2016, May 2016, Art. no. 4073584, doi: [10.1155/2016/4073584](https://doi.org/10.1155/2016/4073584).

[7] R. Maskeliūnas, T. Blazauskas, and R. Damasevicius, “Depression behavior detection model based on participation in serious games,” in *Proc. Int. Joint Conf. Rough Sets (IJCRS)*, 2017, pp. 423–434, doi: [10.1007/978-3-319-60840-2_31](https://doi.org/10.1007/978-3-319-60840-2_31).

[8] I. Martišius and R. Damaševičius, “A prototype SSVEP based real time BCI gaming system,” *Comput. Intell. Neurosci.*, vol. 2016, Jan. 2016, Art. no. 3861425, doi: [10.1155/2016/3861425](https://doi.org/10.1155/2016/3861425).

[9] R. Maskeliūnas, R. Damaševičius, I. Martišius, and M. Vasiljevas, “Consumer-grade EEG devices: Are they usable for control tasks?” *PeerJ*, vol. 4, p. e1746, Mar. 2016, doi: [10.7717/peerj.1746](https://doi.org/10.7717/peerj.1746).

[10] D. A. James and N. Petrone, *Sensors and Wearable Technologies in Sport: Technologies, Trends and Approaches for Implementation*. Singapore: Springer, 2016.

[11] M. Elgendi, E. Mohamed, and R. Ward, “Efficient ECG compression and QRS detection for E-health applications,” *Sci. Rep.*, vol. 7, no. 1, p. 459, 2017, doi: [10.1038/s41598-017-00540-x](https://doi.org/10.1038/s41598-017-00540-x).

[12] D. C. Peritz, A. Howard, M. Ciocca, and E. H. Chung, “Smartphone ECG aids real time diagnosis of palpitations in the competitive college athlete,” *J. Electrocardiol.* vol. 48, no. 5, pp. 896–899, 2015, doi: [10.1016/j.jelectrocard.2015.07.010](https://doi.org/10.1016/j.jelectrocard.2015.07.010).

[13] J. L. Park, M. M. Fairweather, and D. I. Donaldson, “Making the case for mobile cognition: EEG and sports performance,” *Neurosci. Biobehav. Rev.*, vol. 52, pp. 117–130, May 2015, doi: [10.1016/j.neubiorev.2015.02.014](https://doi.org/10.1016/j.neubiorev.2015.02.014).

[14] S. Debener, F. Minow, R. Emkes, K. Gandras, and M. de Vos, “How about taking a low-cost, small, and wireless EEG for a walk?” *Psychophysiology*, vol. 49, no. 11, pp. 1617–1621, 2012, doi: [10.1111/j.1469-8986.2012.01471.x](https://doi.org/10.1111/j.1469-8986.2012.01471.x).

[15] M. de Vos, K. Gandras, and S. Debener, “Towards a truly mobile auditory brain–computer interface: Exploring the P300 to take away,” *Int. J. Psychophysiol.*, vol. 91, no. 1, pp. 46–53, 2014.

[16] T. Thompson, T. Steffert, T. Ros, J. Leach, and J. Gruzeliier, “EEG applications for sport and performance,” *Methods*, vol. 45, no. 4, pp. 279–288, 2008, doi: [10.1016/j.ymeth.2008.07.006](https://doi.org/10.1016/j.ymeth.2008.07.006).

[17] J. E. Kline, H. J. Huang, K. L. Snyder, and D. P. Ferris, “Isolating gait-related movement artifacts in electroencephalography during human walking,” *J. Neural Eng.*, vol. 12, no. 4, p. 046022, 2015, doi: [10.1088/1741-2560/12/4/046022](https://doi.org/10.1088/1741-2560/12/4/046022).

[18] K. L. Snyder, J. E. Kline, H. J. Huang, and D. P. Ferris, “Independent component analysis of gait-related movement artifact recorded using eeg electrodes during treadmill walking,” *Frontiers Hum. Neurosci.*, vol. 9, p. 639, Dec. 2015, doi: [10.3389/fnhum.2015.00639](https://doi.org/10.3389/fnhum.2015.00639).

[19] J. T. Gwin, K. Gramann, S. Makeig, and D. P. Ferris, “Removal of movement artifact from high-density EEG recorded during walking and running,” *J. Neurophysiol.*, vol. 103, no. 6, pp. 3526–3534, 2010, doi: [10.1152/jn.00105.2010](https://doi.org/10.1152/jn.00105.2010).

[20] K. Cao, Y. Guo, and S. W. Su, “A review of motion related EEG artifact removal techniques,” in *Proc. Int. Conf. Sens. Technol. (ICST)*, Dec. 2016, pp. 600–604, doi: [10.1109/ICST.2015.7438469](https://doi.org/10.1109/ICST.2015.7438469).

[21] P. M. Reis, F. Hebenstreit, F. Gabsteiger, V. von Tscharnner, and M. Lochmann, “Methodological aspects of EEG and body dynamics measurements during motion,” *Frontiers Hum. Neurosci.*, vol. 8, p. 156, Mar. 2014, doi: [10.3389/fnhum.2014.00156](https://doi.org/10.3389/fnhum.2014.00156).

[22] K. Gramann, D. P. Ferris, J. Gwin, and S. Makeig, “Imaging natural cognition in action,” *Int. J. Psychophysiol.*, vol. 91, no. 1, pp. 22–29, 2014, doi: [10.1016/j.ijpsycho.2013.09.003](https://doi.org/10.1016/j.ijpsycho.2013.09.003).

- [23] R. Vigário, V. Jousmäki, M. Hämäläinen, R. Hari, and E. Oja, "Independent component analysis for identification of artifacts in magnetoencephalographic recordings," in *Proc. Adv. Neural Inf. Process. Syst.* Cambridge, MA, USA: MIT Press, 1998, pp. 229–235.
- [24] K. Gramann, J. T. Gwin, N. Bigdely-Shamlo, D. P. Ferris, and S. Makeig, "Visual evoked responses during standing and walking," *Frontiers Hum. Neurosci.*, vol. 4, p. 202, Oct. 2010, doi: [10.3389/fnhum.2010.00202](https://doi.org/10.3389/fnhum.2010.00202).
- [25] T. P. Jung et al., "Removing electroencephalographic artifacts by blind source separation," *Psychophysiology*, vol. 37, no. 2, pp. 163–178, 2000, doi: [10.1111/1469-8986.3720163](https://doi.org/10.1111/1469-8986.3720163).
- [26] K. T. Sweeney, S. F. McLoone, and T. E. Ward, "The use of ensemble empirical mode decomposition with canonical correlation analysis as a novel artifact removal technique," *IEEE Trans. Biomed. Eng.*, vol. 60, no. 1, pp. 97–105, Jan. 2013, doi: [10.1109/TBME.2012.2225427](https://doi.org/10.1109/TBME.2012.2225427).
- [27] T. Mullen et al., "Real-time modeling and 3D visualization of source dynamics and connectivity using wearable EEG," in *Proc. 35th Ann. Int. Conf. IEEE Eng. Biol. Med. Soc.*, Jul. 2013, pp. 2184–2187, doi: [10.1109/EMBC.2013.6609968](https://doi.org/10.1109/EMBC.2013.6609968).
- [28] X. Ning, I. W. Selesnick, and L. Duval, "Chromatogram baseline estimation and denoising using sparsity (BEADS)," *Chemometrics Intell. Lab. Syst.*, vol. 139, pp. 156–167, Dec. 2014, doi: [10.1016/j.chemolab.2014.09.014](https://doi.org/10.1016/j.chemolab.2014.09.014).
- [29] S.-C. Pei and C.-C. Tseng, "Elimination of AC interference in electrocardiogram using IIR notch filter with transient suppression," *IEEE Trans. Biomed. Eng.*, vol. 42, no. 11, pp. 1128–1132, Nov. 1995, doi: [10.1109/10.469385](https://doi.org/10.1109/10.469385).
- [30] R. Verma, R. Mehrotra, and V. Bhateja, "An integration of improved median and morphological filtering techniques for electrocardiogram signal processing," in *Proc. 3rd IEEE Int. Adv. Comput. Conf.*, Feb. 2013, pp. 1223–1228, doi: [10.1109/IAdCC.2013.6514402](https://doi.org/10.1109/IAdCC.2013.6514402).
- [31] A. Elbuni, S. Kanoun, M. Elbuni, and N. Ali, "ECG parameter extraction algorithm using (DWTAE) algorithm," in *Proc. Int. Conf. Comput. Technol. Develop.*, Dec. 2009, pp. 57–62, doi: [10.1109/ICCTD.2009.103](https://doi.org/10.1109/ICCTD.2009.103).
- [32] M. Karam, H. F. Khazaal, H. Aglan, and C. Cole, "Noise removal in speech processing using spectral subtraction," *J. Signal Inf. Process.*, vol. 5, pp. 32–41, May 2014.
- [33] T. Blažauskas, A. Muliulis, L. Bikulčiene, and E. Butkevičiūtė, "Service-oriented architecture solution for ECG signal processing," *Inf. Technol. Control*, vol. 46, no. 4, pp. 445–458, 2018, doi: [10.5755/joi.ita.46.4.18470](https://doi.org/10.5755/joi.ita.46.4.18470).
- [34] N. E. Huang et al., "Review of empirical mode decomposition," *Proc. SPIE*, vol. 4391, pp. 71–80, Mar. 2001, doi: [10.1117/12.421232](https://doi.org/10.1117/12.421232).
- [35] Y. Xin, Y. Chen, and W. T. Hao, "ECG baseline wander correction based on mean-median filter and empirical mode decomposition," *Bio-Med. Mater. Eng.*, vol. 24, no. 1, pp. 365–371, 2014, doi: [10.3233/BME-130820](https://doi.org/10.3233/BME-130820).
- [36] M. P. Tarvainen, P. O. Ranta-aho, and P. A. Karjalainen, "An advanced detrending method with application to HRV analysis," *IEEE Trans. Biomed. Eng.*, vol. 49, no. 2, pp. 172–175, Feb. 2002, doi: [10.1109/10.979357](https://doi.org/10.1109/10.979357).
- [37] J. Pan and W. J. Tompkins, "A real-time QRS detection algorithm," *IEEE Trans. Biomed. Eng.*, vol. BME-32, no. 3, pp. 230–236, Mar. 1985, doi: [10.1109/TBME.1985.325532](https://doi.org/10.1109/TBME.1985.325532).
- [38] M. K. Aneja, B. Singh, J. S. Ubhi, and S. Rani, "Digital filtration of ECG signals for removal of baseline drift," in *Proc. Int. Conf. Telecommun. Technol. Appl.*, 2011, pp. 105–109.
- [39] I. W. Selesnick, H. L. Graber, D. S. Pfeil, and R. L. Barbour, "Simultaneous low-pass filtering and total variation denoising," *IEEE Trans. Signal Process.*, vol. 62, no. 5, pp. 1109–1124, Mar. 2014, doi: [10.1109/TSP.2014.2298836](https://doi.org/10.1109/TSP.2014.2298836).
- [40] P. Qui and K. J. R. Liu, "A robust method for QRS detection based on modified P-spectrum," in *Proc. IEEE Int. Conf. Acoust., Speech Signal Process.*, Mar./Apr. 2008, pp. 501–504, doi: [10.1109/ICASSP.2008.4517656](https://doi.org/10.1109/ICASSP.2008.4517656).
- [41] H. Sedghamiz and D. Santonocito, "Unsupervised detection and classification of motor unit action potentials in intramuscular electromyography signals," in *Proc. 5th IEEE Int. Conf. E-Health Bioeng. (EHB)*, Nov. 2015, pp. 1–6, doi: [10.1109/EHB.2015.7391510](https://doi.org/10.1109/EHB.2015.7391510).
- [42] B.-U. Kohler, C. Hennig, and R. Orglmeister, "The principles of software QRS detection," *IEEE Eng. Med. Biol.*, vol. 21, no. 1, pp. 42–57, Jan./Feb. 2002, doi: [10.1109/51.993193](https://doi.org/10.1109/51.993193).
- [43] J. C. Principe, V. Euliano, and W. C. Lefebvre, *Neural and Adaptive Systems: Fundamentals Through Simulations*. Hoboken, NJ, USA: Wiley, 2000.
- [44] S. Kadambe, R. Murray, and G. F. Boudreaux-Bartels, "Wavelet transform-based QRS complex detector," *IEEE Trans. Biomed. Eng.*, vol. 46, no. 7, pp. 838–848, Jul. 1999, doi: [10.1109/10.771194](https://doi.org/10.1109/10.771194).
- [45] V. X. Afonso, W. J. Tompkins, T. Q. Nguyen, and S. Luo, "ECG beat detection using filter banks," *IEEE Trans. Biomed. Eng.*, vol. 46, no. 2, pp. 192–202, Feb. 1999, doi: [10.1109/10.740882](https://doi.org/10.1109/10.740882).
- [46] T. Maiwald, E. Mammen, S. Nandi, and J. Timmer, "Surrogate data—A qualitative and quantitative analysis," in *Mathematical Methods in Signal Processing and Digital Image Analysis (Understanding Complex Systems)*. Berlin, Germany: Springer, 2008, pp. 41–74, doi: [10.1007/978-3-540-75632-3_2](https://doi.org/10.1007/978-3-540-75632-3_2).
- [47] D. Prichard and J. Theiler, "Generating surrogate data for time series with several simultaneously measured variables," *Phys. Rev. Lett.*, vol. 73, no. 7, pp. 951–954, 1994, doi: [10.1103/physrevlett.73.951](https://doi.org/10.1103/physrevlett.73.951).
- [48] T. Schreiber and A. Schmitz, "Surrogate time series," *Phys. D, Nonlinear Phenomena*, vol. 142, nos. 3–4, pp. 346–382, 1999, doi: [10.1016/s0167-2789\(00\)00043-9](https://doi.org/10.1016/s0167-2789(00)00043-9).
- [49] G. Haff and S. Nimphius, "Training principles for power," *J. Strength Conditioning Res.*, vol. 34, no. 6, pp. 3–12, 2012, doi: [10.1519/SSC.0b013e31826db467](https://doi.org/10.1519/SSC.0b013e31826db467).



EGLĖ BUTKEVI IŪTĖ received the master's degree in applied mathematics from the Kaunas University of Technology, in 2015, where he is currently pursuing the Ph.D. degree in informatics. He has authored several articles in international journals. Her main academic subjects are electrocardiogram signal processing, training intensity modeling, fatigue evaluation, and decision-making algorithms. She participated in many conferences.



LIEPA BIKUL IENĖ received the Ph.D. degree in physical sciences informatics, in 2007. She is currently an Associate Professor with the Department of Applied Mathematics, Faculty of Mathematics and Natural Sciences, Kaunas University of Technology, Lithuania. She has participated in three international Eureka projects. She has authored more than 60 international and national publications in the fields of mathematical modeling, differential equations, complex systems, and physiological human state evaluation.



TATJANA SIDEKARSKIENĖ received the B.Sc. degree in mathematics from the Faculty of Fundamental Sciences, Kaunas University of Technology (KTU), Kaunas, Lithuania, in 2003, and the M.Sc. degree, in 2006. She is currently an Assistant Professor with the Department of Applied Mathematics, KTU. She lectures mathematics courses. Her main research interests include time series analysis and signal decomposition methods.



TOMAS BLA AUSKAS is currently an Associate Professor with the Department of Software Engineering, Faculty of Informatics, Kaunas University of Technology. He has participated in six international scientific projects. He has authored more than 30 research articles and publications. Virtual reality solutions designed by his research group were demonstrated in more than 20 exhibitions and other events. His scientific interests include multimodal input and output interfaces, smart well-being technologies, augmented and virtual reality systems, and gamification in e-learning.



RYTIS MASKELIŪNAS received the Ph.D. degree in computer science, in 2009. He is currently a Professor with the Department of Multimedia Engineering, Faculty of Informatics, and a Chief Researcher with the Centre of Real Time Computer Systems, Kaunas University of Technology. He has authored or co-authored over 80 refereed scientific articles. His main areas of scientific research are multimodal signal processing, and modeling, development, and analysis of associa-

tive, multimodal interfaces, mainly targeted at elderly and people with major disabilities. He received various awards/honors, including the Best Young Scientist Award, in 2012, and the National Science Academy Award for Young Scholars of Lithuania, in 2010. He serves as a Reviewer/Committee Member for various refereed journals.



ROBERTAS DAMAŠIUS received the Ph.D. degree in informatics engineering from the Kaunas University of Technology (KTU), in 2005. He is currently a Professor with the Software Engineering Department, KTU. He lectures software maintenance, human-computer interface, and robot programming courses. He has authored over 200 papers and a monograph published by Springer. His research interests include sustainable software engineering, human-computer inter-

faces, assisted living, data mining, and machine learning. He has been a Guest Editor for several invited issues of international journals, including *Biomed Research International*, *Computational Intelligence and Neuroscience*, the *Journal of Universal Computer Science*, the IEEE ACCESS, *Mathematical Biosciences and Engineering*, the *Journal of Healthcare Engineering*, and *Computers* (MDPI). He is the Editor-in-Chief of the *Information Technology and Control* journal.



WEI WEI received the M.S. and Ph.D. degrees from Xian Jiaotong University, in 2011 and 2005, respectively. He is currently an Associate Professor with the School of Computer Science and Engineering, Xi'an University of Technology, Xi'an, China. He ran many funded research projects as a Principal Investigator and as a Technical Member. He has published around hundreds of research papers in international conferences and journals. His research interests include wireless networks,

wireless sensor network applications, image processing, mobile computing, distributed computing, pervasive computing, the Internet of Things, and sensor data clouds. He is a Senior Member of the IEEE and CCF. He is also a member of the Editorial Board of FGCS, AHSWN, IEICE, and KSII. He is also a TPC Member for many conferences and a Regular Reviewer of the IEEE TPDS, TIP, TMC, TWC, JNCA, and many other Elsevier journals.

• • •